ORIGINAL PAPER

CrossMark

The effect of reactive diluent on mechanical properties and microstructure of epoxy resins

Morteza Khalina[1] · Mohammad Hosain Beheshty[1] · Ali Salimi[2]

Abstract

The effects of an aliphatic reactive diluent on the viscosity, gel time, chemical resistance, mechanical properties, fracture toughness, microstructure and relaxations of two different epoxy resins, i.e., a bifunctional and a multifunctional epoxy, were investigated. The gel time was not significantly affected by the diluent. The modulus and ultimate strength gradually declined, while the ductility steadily increased as the diluent content was increased. The failure mode of epoxy samples under flexural test changed from brittle to much more ductile upon the progressive incorporation of diluent into the epoxy resins. The strain at break of bifunctional resin improved by 75%, while that of multifunctional resin enhanced by more than 24%. The dynamic mechanical thermal analysis (DMTA) showed that the introduction of reactive diluent into different epoxy resins reduced the storage modulus at the glassy region and significantly broadened the glass transition region of the epoxy matrices with approximately no change in the glass transition temperature. The DMTA results also indicated increased microstructural heterogeneities upon the addition of diluent to the epoxy resins as evidenced by atomic force microscopy. The fracture toughness of epoxy resins enhanced with diluent content, about 20% and 29% increase for bifunctional and multifunctional resins, respectively. This was attributed to the improved material's ductility and activation of plastic deformation in the epoxy resins upon the addition of reactive diluent.

Keywords Reactive diluent · Epoxy resin · Mechanical properties · Toughness · Microstructure

✉ Mohammad Hosain Beheshty
  M.Beheshty@ippi.ac.ir

[1] Department of Composites, Iran Polymer and Petrochemical Institute, 15km Tehran-Karaj Highway, Pajuhesh Science and Technology Park, Pajuhesh Blvd, Tehran, Iran

[2] Department of Resin and Adhesives, Iran Polymer and Petrochemical Institute, Tehran, Iran

🖄 Springer

Introduction

Epoxy resins are widely used as matrix resins for fiber-reinforced composites due to high mechanical strength and modulus, good adhesion property and dimensional stability [1]. However, as a consequence of their highly cross-linked structure, these materials suffer from brittleness, poor crack resistance and low fracture toughness, which limit their applications in certain areas [2, 3]. Therefore, much research has been carried out to enhance the toughness of the cured epoxy resins without any significant loss in other properties [4–6]. Several methods have been proposed for increasing the toughness of epoxy resins, including the use of polysulfones [7, 8], chain branching [9] and fibers [10], and one of the most effective approaches is the introduction of a second component which is capable of phase separation as reactive liquid rubber [11], thermoplastic [12] or core–shell particles [8, 11, 12]. Because of their excellent elasticity and good impact strength, a number of polyol-based reactive diluents have been considered as a good choice to improve the resistance to brittle fracture of epoxy resins [13–15]. In addition to the toughening effect on the epoxy system, lower viscosity and extended pot life increase the resin wetting action and the level of filler loading without substantial decrease in curing rate and thermal stability. These properties make polyols suitable for the modification of an epoxy matrix to obtain improved peel and impact strengths, and facilitate processing of fiber-reinforced polymer composites. Grishchuk et al. [16] used a polyethersulfone as a toughener for epoxy resins. They found 160% improvement in Charpy impact properties. Urbaczewski-Espuche et al. [17] have studied the effect of an aliphatic reactive diluent on the properties of a diglycidyl ether bisphenol-A epoxy (DGEBA) resin. The cross-link density and the chain flexibility increased with the amount of diluent, while the elastic modulus was decreased [18–20]. Fracture toughness was improved as the amount of diluent was increased. Crack propagation was related to the ability of the networks to deform plastically [21–23]. Montserrat et al. [24] studied the effect of a reactive diluent (RD) on the kinetics of the curing of an epoxy resin, based on DGEBA. Increasing the RD content leads to a small increase in both the non-isothermal and the isothermal heats of curing and has a slight effect on the kinetic parameters. The introduction of aliphatic chains in the structure of the epoxy decreased the glass transition temperature. Harani et al. [25] used two types of Desmophen (800 and 1200) as modifiers of epoxy systems. Hydroxyl-terminated polyester, a polyol, improved the epoxy toughness. Polyol type (Mw and branching) and concentration significantly affected the impact strength and critical stress intensity factor of epoxy resins. Desmophen 1200 led to fairly good results. The localized plastic shear yielding was the prevailing toughening mechanism for epoxy resins. Rosu et al. [26] synthesized para-tert-butyl phenol formaldehyde epoxy-acrylic resin and cured in the presence of reactive diluents based on glycidyl ethers of phenol, para-tert-butyl phenol, as well as para-nonylphenol. The analyzed samples heated on 110 °C, duration 16 h, showed that the curing reaction depends very much on the structure of the reactive diluents. Nunez-Regueira et al. [27] used differential scanning calorimetry

to study the influence of an epoxy reactive diluent, vinyl cyclohexane dioxide on the curing reaction of a polymeric system composed of diglycidyl ether of bisphenol A and 1,2-diaminocyclohexane (DCH). Both the curing degree and the glass transition temperature of the polymeric system decrease with an increase in the diluent percentage. Das and Karak [28] used an epoxidized vegetable oil as a reactive diluent for commercial BPA-based epoxy resin at different compositions. The results indicated that the epoxidized oil not only reduces the viscosity of the BPA-based epoxy resin but it also enhances the performance of the cured resin. Bakar et al. [29] modified the epoxy resin using phenyl diglycidyl ether (PGE), xylene and kaolin. The impact strength (IS), critical stress intensity factor (K_C), flexural strength and glass transition temperature (T_g) were evaluated as functions of the modifier content. It was found that the addition of diluents led to a significant reduction in both viscosity and T_g. A threefold increase in IS was obtained with the addition of 2.5% PGE. Moreover, the addition of 15% PGE resulted in about 145% enhancement of the K_C. However, the addition of xylene had no significant effect on these properties. Rahman et al. [30] investigated the morphology and properties of nanotube/polyol/epoxy ternary nanocomposites. The addition of a polyether polyol to the epoxy resin increased Mode-I fracture toughness and flexural strain energy, while adversely affected the flexural strength and stiffness. A synergistic effect was observed with the addition of amino-functionalized multi-walled carbon nanotubes (NH_2-MWCNTs) into polyol-toughened epoxy, with significant improvements in fracture toughness and strain energy as well as in flexural strength and stiffness. Matrix plastic deformation and lower cross-link density due to polyether polyol in the epoxy system increased toughness while reducing flexural strength and stiffness. However, incorporation of 0.3 wt% of NH_2-MWCNTs into the polyol-toughened epoxy composites improved the mechanical properties as well as fracture toughness, compared with pristine epoxy and polyol-toughened epoxy.

In our previous work, we studied the mechanical and fracture resistance properties of blends of two epoxy resins [31]. The present work was aimed to study the structure and properties of epoxy resins modified with a reactive diluent. A comparison study was made using two kinds of epoxy resins. One was a bifunctional epoxy resin, and the other was a multifunctional epoxy resin. Then, the effect of diluent content on the microstructure, mechanical properties, fracture toughness, solvent resistance and cross-link density of the resulting thermoset material was systematically investigated. The novelty of present work is that the effect of epoxy matrix functionality on the ultimate properties of modified epoxy was examined in detail. In addition, the effects of diluent content on the gel time, chemical resistance and compressive mechanical properties are rarely reported in previous works which are investigated in this work. Attempt was made to establish a structure–property correlation in the epoxy systems under investigation.

Experimental

Materials

The epoxy resins with the trade names of LV1189 (Mokarar Co., Iran) and Epikote 828 (Momentive Co., USA) were used in this work, with epoxy equivalent weight (EEW) of 185 g/mol and 182 g/mol, respectively. The viscosity of LV1189 at 80 °C was 2400 mPa s, while the viscosity of Epikote 828 at 25 °C was 12,000 mPa s. The reactive diluent used was 1, 4-butanediol diglycidyl ether (BDDGE) (Mokarar Co., Iran), which is a bifunctional diluent with EEW of 132 g/mol. The viscosity of BDDGE at 25 °C was 14.1 mPa s. HA76 (Mokarar Co., Iran) is an aliphatic amine hardener with amine H equivalent weight (HEW) of 52 g/mol and was purchased and used as a room-temperature curing agent. The viscosity of HA76 at 25 °C was 12.5 mPa s.

LV1189 is a novolac and multifunctional based epoxy resin, which is semisolid at ambient temperature. To measure its viscosity, this resin was first heated up to 80 °C and then, its viscosity was measured at this temperature. Epikote 828 is a general purpose and a bifunctional epoxy resin based on diglycidyl ether bisphenol-A (DGEBA), but its viscosity at room temperature is high for many applications.

Formulations and mixtures

Epikote 828 is a liquid resin, and LV1189 is a semisolid resin; given the scope of viscosity applicable in various industries, different amounts of diluents were used in the formulation of these two resins to maintain the viscosity of the mixtures at ambient temperatures in the range of 700–1300 mPa s in the final mixture. The EEW of mixture (EEW_{mix}) was calculated from the following equation.

$$EEW_{mix} = \frac{W_{mix}}{\frac{W_a}{EEW_a} + \frac{W_b}{EEW_b} + \cdots} \qquad (1)$$

where W_i and EEW_i are the weight and EEW of component i in the mixture, respectively. The amount of curing agent (CA) required per 100 g of resin mixture under the stoichiometric conditions was calculated by the following equation.

$$CA \, (phr) = \frac{\text{Amine H eq wt} \times 100}{EEW_{mix}} \qquad (2)$$

In all the mixtures, 1 ± 0.5 phr extra curing agent was added to complete the curing reaction. The amounts of resin, diluents and curing agent used as well as the coding of the samples are shown in Table 1.

Table 1 Formulations of different epoxy samples prepared in this work

Sample code	Epikote 828 (phr)	LV1189 (phr)	BDDGE (phr)	EEW (g/mol)	HA 76 (phr)
E0	100	0	0	189	28.6
E15	100	0	15	173.4	30.0
E20	100	0	20	171.2	30.4
E25	100	0	25	169.2	30.7
E30	100	0	30	167.4	32.1
L0	0	100	0	185	28.1
L30	0	100	30	169.3	31.7
L50	0	100	50	163.2	31.9
L60	0	100	60	160.8	32.3
L70	0	100	70	158.8	32.8

Mixing and curing procedures

At first, the raw resin was weighed for each sample and modified by the addition of a predetermined amount of diluent. Due to the high viscosity of LV1189 at ambient temperature, it was heated up to 80 °C for 10 min and then was mixed with predetermined weight of reactive diluent. The resin–diluent mixtures were blended by a mechanical mixer running at 400 rpm for 20 min to obtain a homogenous mixture. Then, the mixture cooled down to the room temperature. In the next stage, the curing agent was added to the resin–diluent system and was mixed for 15 min by a mechanical mixer running at the same speed. At the end of mixing process and to remove the trapped bubbles, the mixture was placed in a vacuum oven at 25 °C for 10 min.

The mixtures of different samples were molded in a silicone mold. Then, the samples were cured at ambient temperature for 24 h and finally post-cured at 80 °C for 4 h to complete the curing process.

Test procedures

Viscosity measurement

A Brookfield RVDV-II-Pro rotational viscometer was employed for viscosity measurements according to ASTM D2196 standard. To do this, about 3 mL of the sample was placed in the device's cup of spindle No. 14 and after reaching the desired torque and temperature, the sample's viscosity was measured.

Measurement of epoxy equivalence weight (EEW)

The EEW of neat resins and also some mixtures was measured according to ASTM D1652-04 standard. For this purpose, the resin was first dissolved in an

appropriate diluent such as di-chloromethane and then, the resulting solution was reacted in directly or inversely titration by hydrogen bromide. There was a good agreement between the measured EEWs and the calculated ones (according to Eq. (1)) for resin mixtures.

Determination of gel time

Gel time of the samples was determined according to ISO 8130-6 standard test method. About 2 mL of the sample was placed on a metal hot plate at the desired temperature. The gel time of the samples was recorded at two different temperatures of 25 and 60 °C. During the test period, the sample was stirred continuously with a glass rod. The resin viscosity increased gradually due to cross-linking, and after a while, it showed an elastic behavior (like a gel) and reached the gel state. At this time, the timer was stopped and the recorded time was reported as the gel time. The experiment was repeated at least three times for each sample and at each temperature.

Chemical resistance

The chemical resistance of the samples was determined in acetone and methyl ethyl ketone (MEK) solvents. A rectangular cubic of cured sample with the dimension of $75 \times 25 \times 3.2$ mm^3 was prepared, and its weight was measured after complete curing and drying. The specimen was then immersed in acetone or MEK solvents at room temperature, and the change in weight of the sample was measured after 24-h immersion.

Mechanical properties

The mechanical properties of the samples were measured under the compression and flexural tests according to ASTM D695 and ASTM D790 standards, respectively. For flexural properties, specimens with the dimension of $80 \times 13 \times 3.2$ mm^3 were prepared and subjected to a three-point bending test using a SANTAM STM-I50 universal testing machine (UTM). In the case of compression test, the specimens with the dimension of $13 \times 13 \times 20$ mm^3 were prepared and subjected to compression test. The mechanical tests were carried out at room temperature. The reported mechanical properties are the average of at least four repetitions.

Dynamic mechanical thermal analysis (DMTA)

DMTA test was used to study the viscoelastic properties of some samples, according to ASTM D5023 standard. The glass transition temperature of the cured samples was determined form the peak of tan δ curve. Rectangular specimens of $30 \times 12.5 \times 3.2$ mm^3 dimension were cut from the molded sheets and were tested using a Triton (model Tritec 2000 DMA, UK) instrument. The DMTA test was

performed at a frequency of 1 Hz, temperature range of 30–160 °C and at a heating rate of 5 °C/min.

Fracture toughness measurement

The three-point single-edge notched bending (SENB) specimens were used to measure the fracture toughness of the samples according to ASTM D5045 standard. Rectangular specimens of approximately $57 \times 12.7 \times 6.4$ mm^3 were prepared; a notch of about 2 mm depth was inserted using a fresh saw, and then, a line of 1.0 mm depth was drawn in the notch root with a frozen fresh razor blade. For this purpose, a frozen sharp blade was tapped on the notch root such that a natural crack forms at the tip of the notch. The samples were then tested using a SAN-TAM machine operated at a bending speed of 10 mm/min at room temperature.

The plane-strain critical stress intensity factor (K_{IC}), as a measure of fracture toughness, was calculated using the following equations:

$$K_{IC} = \frac{P_Q}{BW^{\frac{1}{2}}} f(x)$$ (3)

$$f(x) = 6\sqrt{x} \frac{\left[1.99 - x(1-x)\left(2.15 - 3.93x + 2.7x^2\right)\right]}{(1+2x)(1-x)^{\frac{3}{2}}}$$ (4)

where P_Q is the critical load for expansion of the sharp pre-crack, B is the sample thickness, W is the sample width and $f(x)$ is a dimensionless constant (shape factor) that depends on the geometry and mode of loading. Moreover, $x = \frac{a}{w}$ where a is the pre-crack length and w is the width of specimen.

The fractured surfaces of the samples were examined via atomic force microscopy (AFM) (C26 model, DME Co., Denmark) and scanning electron microscopy (SEM, VEGA Tescan model) techniques. The mode of failure and mechanisms of deformations of different samples were studied and proposed by the observation of fractured surface morphology.

Phase morphology

The phase morphology of the samples was investigated by scanning electron microscopy (SEM, VEGA Tescan model) technique. The samples were cryo-fractured in liquid nitrogen and then coated with a thin layer of gold prior to microscopic imaging.

Table 2 Viscosity and gel time of E- and L-type epoxy series

Sample code	Viscosity (mPa s) at 30 °C	Viscosity (mPa s) at 60 °C	Gel time (min) at 25 °C	Gel time (min) at 60 °C
E0	11,500 ± 25	1250 ± 25	60 ± 5	40 ± 5
E15	950 ± 25	150 ± 12	55 ± 5	35 ± 5
E20	700 ± 25	125 ± 12	65 ± 5	40 ± 5
E25	562 ± 12	62 ± 12	50 ± 5	30 ± 5
E30	475 ± 12	37 ± 12	50 ± 5	30 ± 5
L0	Semi solid	2200 ± 25	–	55 ± 5
L30	2300 ± 25	275 ± 25	120 ± 5	60 ± 5
L50	1375 ± 25	200 ± 25	115 ± 5	55 ± 5
L60	812 ± 25	175 ± 12	130 ± 5	60 ± 5
L70	600 ± 12	105 ± 12	120 ± 5	55 ± 5

Results and discussion

Determination of viscosity

The viscosities of E- and L-based epoxy samples (Table 1) containing different amounts of reactive diluent were measured at the temperatures of 30 °C and 60 °C, and the results are listed in Table 2. As expected, the viscosity of the epoxy samples gradually decreased as the content of reactive diluent in the epoxy samples was increased, regardless of the type of epoxy matrix. This is due to dilution effect of the diluent on the epoxy samples which tends to increase the molecular weight between the cross-linking points via decreasing the cross-link density of the diluted epoxy sample (see following sections). Moreover, an increase in test temperature from 30 to 60 °C led to a significant reduction in epoxy sample's viscosity, as expected. At a given diluent content (30 phr), the viscosity of L-based epoxy sample is greater than that of E-based sample which is due to the higher viscosity of neat LV1189 epoxy resin than the neat Epikote 828 resin.

Gel time

The gel times of E- and L-based epoxy samples were measured at ambient temperature (25 ± 1 °C) and 60 °C. The average values of gel times of different epoxy mixtures are summarized in Table 2. No clear trend can be seen in this table for the effect of diluent content on the gel time of epoxy samples of different chemical structures. The level of scattering of data obtained at 60 °C is much less than that at 25 °C. Therefore, it can be concluded that an increase in the amount of diluent in the range studied in this work does not significantly affect the gel time of the epoxy mixtures. However, it is obvious from the data in Table 2 that an increase in test temperature from 25 to 60 °C accelerated the gelation process in the epoxy samples, so that a remarkable decline in the gel time is clearly apparent
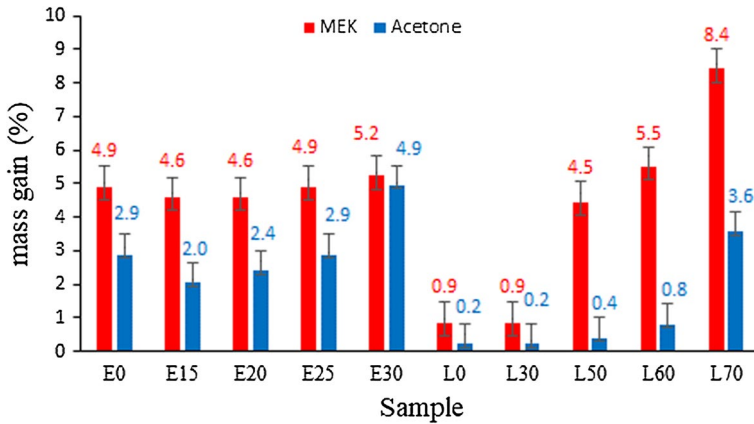
Fig. 1 Mass gain for different epoxy samples in the presence of acetone and MEK solvents

for epoxy samples as the temperature was increased. This is because the cross-linking reactions accelerate as the test temperature was increased. In other words, the increase in temperature reduces the activation energy for cure reactions in the epoxy samples.

Chemical resistance

To determine the chemical resistance of the epoxy samples, the change in the mass of samples immersed in the active solvents for 24 h was calculated and the results are presented in Fig. 1. In the case of E-based epoxy samples containing various amounts of diluent, the data in Fig. 1 demonstrate that the amount of mass gain in the MEK solvent slightly increases with the diluent concentration in the epoxy system. The same trend can be observed for E-based epoxy samples in the acetone solvent, in that the extent of mass gain of resulting epoxy increases with the weight fraction of diluent in the sample.

For L-based epoxy samples, the data reveal an enhanced mass gain with diluent content in both MEK and acetone solvents. The chemical resistance data further indicate that both L- and E-based epoxy samples are much less resistant to MEK solvent than the acetone solvent. The change in mass gain as a function of diluent content is probably due to the change in the microstructure (molecular weight between entanglements and cross-linking density) of epoxy samples as a result of the incorporation of diluent in these samples (see following section). Moreover, at the same level of diluent loading (i.e., 30 phr), the L-based epoxy sample is considerably more resistant against acetone and MEK solvents than the E-based sample. This is due to the fact that L-type epoxy is a multifunctional epoxy sample while the E-type epoxy is a bifunctional one. The higher cross-link density of L-type epoxy as compared with the E-type sample is responsible for its much lower mass gain in both solvents.

Cross-link density measurements

The cross-link density (CLD) of the samples was measured from chemical resistance and swelling results in acetone solvent. The CLD of the epoxy samples, μ, was measured from the Flory–Rehner equation [32]:

$$\mu = \frac{-\left[\ln(1-v) + v + \chi v^2\right]}{V\left[v^{1/3} - \frac{v}{2}\right]} \tag{5}$$

where v is the volume fraction of polymer in the swollen gel at equilibrium, χ is the polymer–solvent interaction parameter and V is the molar volume of solvent. The volume fraction of polymer (v) can be calculated from the equation [32, 33]:

$$v = \frac{m_1 d_s}{m_1(d_s - d_p) + m_2 d_p} \tag{6}$$

where m_1 is the weight of polymer before swelling, m_2 is the weight of the polymer after swelling, d_s is the density of solvent and d_p is the density of polymer. The polymer–solvent interaction parameter (χ) was determined by the following relation [32]:

$$\chi = \beta_1 + \left(V/_{RT}\right)(\delta_s - \delta_p)^2 \tag{7}$$

where β_1 is the lattice constant, usually about 0.34, V is the molar volume of solvent, R is the universal gas constant, T is the absolute temperature, δ is the
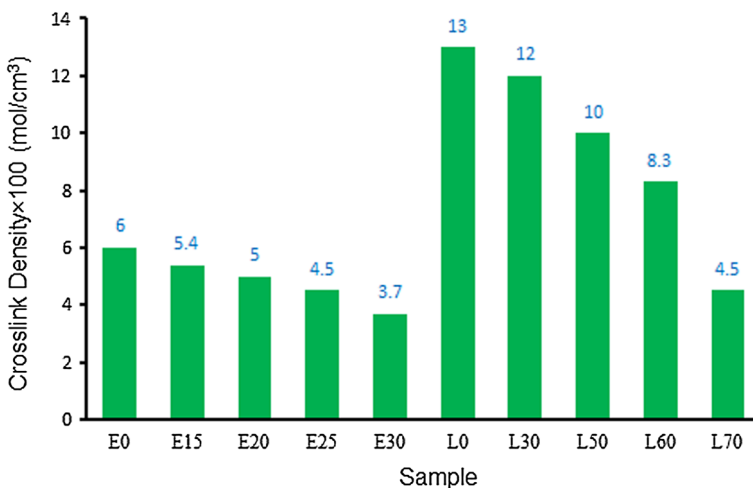

Fig. 2 Cross-link density (CLD) of different samples determined from swelling tests in acetone solvent

solubility parameter and the subscripts *s* and *p* refer to the swelling agent and polymer, respectively.

The results for CLD of the different epoxy samples prepared in this work are presented in Fig. 2.

As can be seen in Fig. 2, the CLD of E-type epoxy samples is significantly higher than that of L-type samples. Moreover, the data demonstrate that the CLD values for both E- and L-type epoxy samples gradually decreased as the reactive diluent content in the epoxy samples was increased. This finding is in line with the result reported in the literature [27, 30]. The reduction in CLD for samples with diluent content can be attributed to the plasticization effect of diluent which tend to increase the molecular weight between entanglements. As a result, the CLD tends to fall as the concentration of diluent was increased.

It should be noted that the results of CLD measurements are consistent with the results given in Fig. 1, in that the E-type epoxy samples showed greater mass gain than the L-type samples in acetone solvent as the CLD of the former samples is lower than that of the latter ones.

Flexural properties

The typical flexural stress–strain curves of pure epoxies (E0 and L0 types) along with the different E- and L-based epoxy samples containing various amounts of reactive diluent are shown in Fig. 3. The progressive introduction of higher loadings of reactive diluent changed the stress–strain response of epoxy samples in the similar way. The L0 epoxy showed a linear elastic response with low ultimate strength and ductility, while the E0 epoxy sample exhibited nonlinear stress–strain behavior with much greater ultimate strength and strain at break.

As can be seen in Fig. 3, the gradual increase in the weight fraction of diluent in the both E- and L-type epoxies changed the flexural behavior of the epoxy material from brittle type into more ductile one. An increase in diluent content from 15 to 20 phr altered the response of the epoxy material to much more ductile. Further increase in the concentration of diluent in the E-base epoxy sample from 20 to 30 gradually reduced the maximum stress and ultimate strength of the resultant material with no change in the strain at break.

In the case of L-type epoxy samples, the stress–strain curves in Fig. 3 show that L30 sample fails in a brittle manner. The other L-type epoxy samples with higher diluent content exhibited much more ductility under the flexural test, which is manifested in the much larger strain at break values of these samples. It seems that a steady increase in the content of diluent in the L-based epoxies gradually reduces the maximum stress and ultimate strength of the samples. The changes in tensile behavior of epoxy samples with diluent content can be ascribed to the change in the CLD of the samples as a consequence of addition of diluent to samples. Lower CLD values are more favorable to greater material's deformation and deviation from linear elastic response.

Compared to E-based epoxy samples, the L-type epoxy samples display lower ductility even at higher diluent content. This may be due to the much higher network
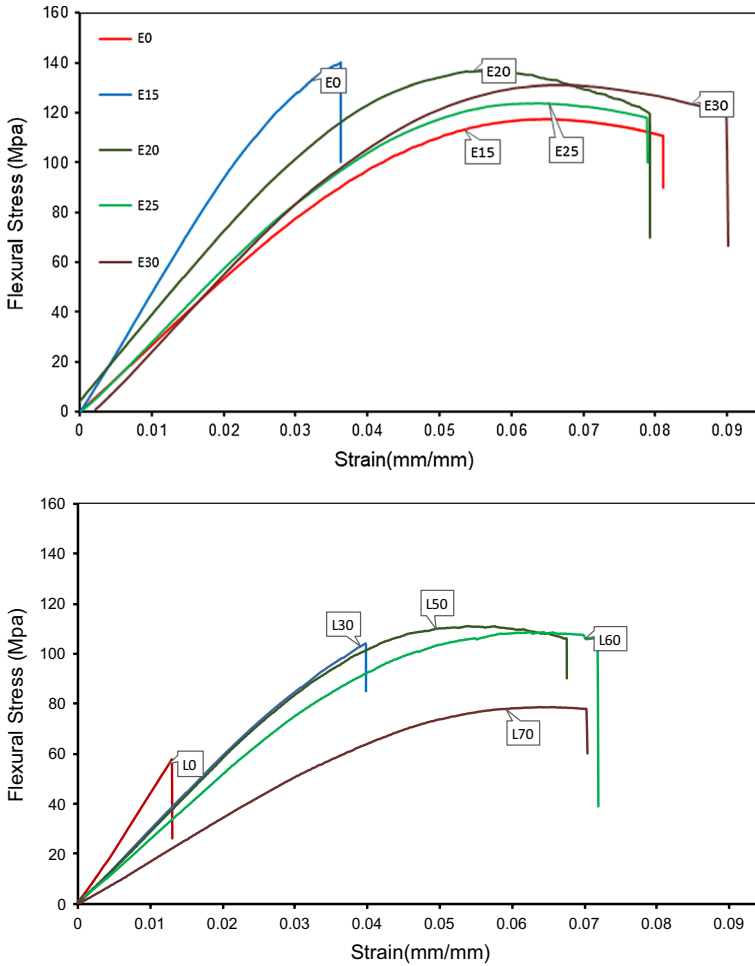
Fig. 3 Typical stress–strain curves of E- and L-type samples modified with various amounts of reactive diluent

cross-link density in the L-type epoxy samples than the E-type ones (see Fig. 2), which restricts the material's deformability under the flexural test.

The different flexural properties of the epoxy samples were measured from the curves of Fig. 3, and the results are depicted in Fig. 4. In the case of L-based epoxy samples, it is apparent that the L0 sample had much higher flexural modulus at the cost of significantly lower flexural strength and deflection at break compared with the other samples. For E-based epoxy samples, the flexural properties of E0 sample are comparable with those of its modified versions.

As can be seen in Fig. 4, the flexural modulus of epoxy samples decreased with the diluent content in the sample, regardless of the type of epoxy matrix. An increase in the weight fraction of reactive diluent declines the material's resistance against
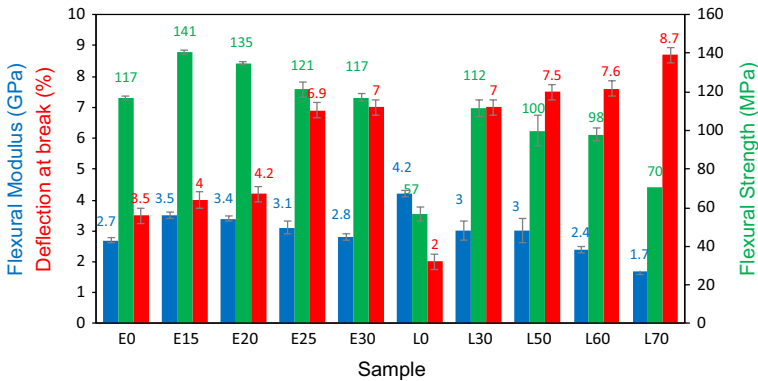
Fig. 4 Flexural properties (flexural modulus, flexural strength and deflection at break) of epoxy samples containing different amounts of reactive diluent

deformation under flexural test, as expected. This is due to the plasticizing effect of diluent used in the epoxy samples in this work which reduces the stiffness of the epoxy material [17–19]. The higher the content of diluent in the epoxy sample, the lower the stiffness of resultant material [17–19]. The same trend can be observed for flexural strength of epoxy samples as a function of diluent content (Fig. 4). This is because the ultimate strength of the material is also dependent on the rigidity of the epoxy material [19, 20].

For strain at break parameter, the results in Fig. 4 demonstrate that for E-type epoxies, the material's ductility significantly increases at first for the sample containing 20 phr of reactive diluent compared to the sample with 15 phr diluent and then remains almost unchanged for the samples with higher loadings of diluent. For L-type epoxy samples, the strain at break enhances with diluent content up to sample with 60 phr diluent and then slightly decreased for the sample containing 70 phr diluent. The increase in deflection at break is due to the increase in material's flexibility upon the incorporation of reactive diluent, which in turn enhances the deformability under the flexural test. The higher the content of diluent in the epoxy sample, the greater the flexibility and deformability of resultant material.

In addition to the plasticizing effect of diluent in the epoxy samples, the fall in the CLD of the epoxy samples upon the addition of diluent is also responsible for the increase in deflection at break and a decrease in strength and stiffness (modulus) of modified epoxies in Fig. 4.

Compression strength

The compressive strength of the epoxy samples is displayed in Fig. 5. For E-type epoxy samples, the compressive strength slightly decreased with the diluent content in the epoxy sample. This finding is in agreement with the literature [18–20]. In the case of L-type epoxies, the samples containing higher than 30 phr of diluent exhibited much lower compressive strength than the sample with 30 phr diluent. Nonetheless, the L-type epoxy samples with 50–70 phr diluent show approximately the same
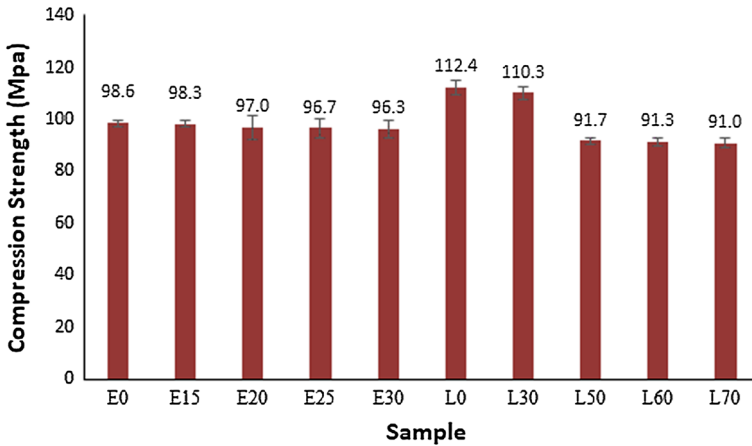
Fig. 5 Compression strength of different epoxy samples

compressive strength. It can be said that increasing the amount of diluent does not affect the compressive strength which may be due to the fact that shear failure is the main mechanism of failure in compression test. The decline in compressive strength with diluent content is partly due to reduced CLD values of epoxy samples containing progressively higher loadings of diluent.

DMTA results

The DMTA results of some of epoxy samples are shown in Fig. 6. This figure shows the temperature dependence of storage modulus and loss tangent for E15, E25, L50 and L70 epoxy samples. The storage modulus is related to the elastic response of the
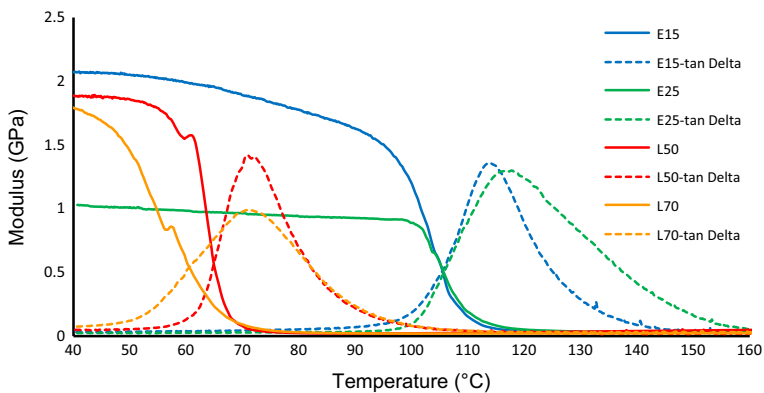

Fig. 6 Temperature dependence of dynamic viscoelastic parameters (storage modulus and loss tangent) for E15, E25, L50 and L70 samples

material, while the loss tangent is associated with the relaxation processes occurring in the sample [24].

The storage modulus gradually declines with temperature, and a sudden fall in the storage modulus can be seen at a defined temperature for epoxy samples illustrated in Fig. 6. In the case of loss factor, a peak can be observed. This peak was considered as the glass transition temperature of epoxy sample under investigation. In the case of storage modulus of E15 and E25 epoxy samples, it can be seen that increase in the diluent content from 15 to 25 phr mostly affected the storage modulus curves of the samples at the glassy state regions. A remarkable drop in storage modulus value at the glassy region is clearly visible for E25 sample compared with E15, undoubtedly due to the higher content of reactive diluent in the former sample than the latter one [24]. The lower CLD value of E25 sample compared with E15 sample may also partly contribute to the lower modulus of E25 than the E15 one (see Fig. 2). No significant change was detected for glass transition temperature of E25 sample compared with E15 one. In turn, the loss factor curve reveals that the relaxation peak of E25 is much broader compared with the E15 sample. This broadening is extended toward higher temperatures. This indicates that the epoxy sample composed of 25 phr diluent contains higher degree of microstructural heterogeneities than the sample with 15 phr diluent [27–29]. This finding indicates that an increase in diluent content from 15 to 25 wt% led to an increase in the microstructural heterogeneities in the modified E-type epoxy systems.

The effect of diluent content on the dynamic viscoelastic properties of L50 and L70 samples is the same as that observed for E-based epoxy samples discussed above (Fig. 6). It is apparent that the L70 sample has lower storage modulus than the L50 sample at the glassy state region, most probably due to the higher diluent content followed by lower CLD of the former sample than those for the latter one (see Fig. 2). Moreover, the relaxation peak of L70 sample is much broader than the L50 sample. It can be seen that the presence of higher contents of reactive diluent activated the relaxation processes at lower temperatures compared with the L50 sample. However, the relaxation peak corresponding to the glass transition temperature of L70 sample did not change as compared with L50 sample. Moreover, higher amount of diluent produced higher degree of microstructural heterogeneities compared with the L50 sample, which is manifested by a much broader relaxation transition as compared with the L50 sample. While many studies in the literature reported a decrease in the glass transition temperature with the addition of diluent into the epoxy resins, the results of the present work reveal no significant change in the glass transition temperature and just a significant broadening of the relaxation peak was detected. In turn, the DMTA results of the present work show considerably enhanced microstructural heterogeneities in the diluted epoxies studied in this work.

Phase morphology

The SEM micrographs taken from cryo-fractured surfaces of some of epoxy samples are shown in Fig. 7. For E-based epoxy samples, the morphological textures observed for samples containing various amounts of diluent are similar to each
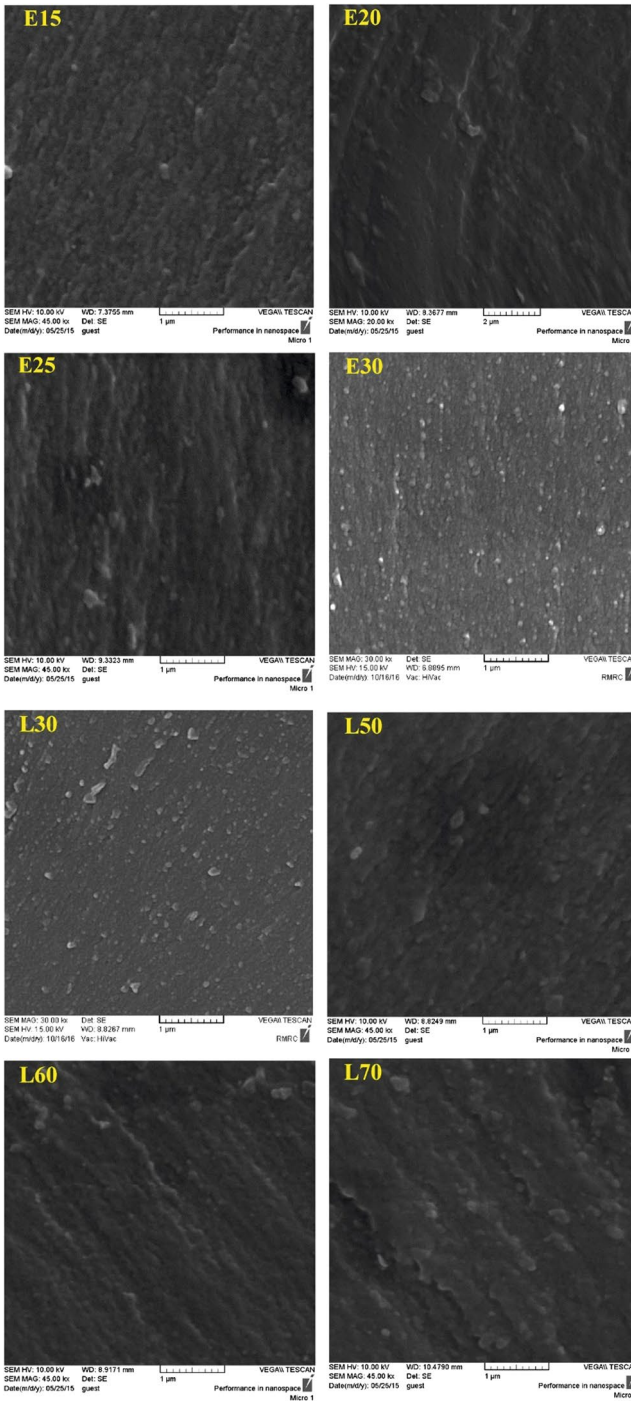
Fig. 7 SEM micrographs taken from the cryo-fractured surfaces of some of E- and L-type epoxy samples containing various amounts of reactive diluent

other. The SEM micrographs reveal the presence of numerous submicron spherical structures (particles) in the structure of E-based epoxy samples. The SEM micrographs of cryo-fractured surfaces of some of L-based epoxy samples are also shown in Fig. 7. The structural characteristics visible in the micrographs for L-based samples are similar to what observed for E-based epoxies. The inhomogeneities are related to the diluent in the epoxy systems, which are present in the epoxy resins in relatively large concentrations. At relatively high concentration of diluent in these epoxy samples, the diluent component can form separate domains and/or phases in the epoxy mixtures. It seems that the amount of microstructural heterogeneities increases with the diluent content in the samples as the higher number and larger inhomogeneities form in the L-based epoxies. This is due to the much higher diluent content in the L-based epoxies as compared with the E-based samples. This increase in the particles' concentration with increasing diluent content further corroborates that the particles are associated with the diluent component in the epoxy resins. Similar morphological textures are also reported in the literature by other researchers for other epoxy systems [25, 34].

Fracture toughness

The typical load–displacement curves of different epoxy samples containing various amounts of reactive diluent are shown in Fig. 8. It can be seen that the shape of load–displacement curves for neat epoxies and the different E- and L-based epoxy samples did not change upon the addition of different amounts of diluent into epoxy resins. However, the maximum load, maximum displacement and the area under the load–displacement curves are affected by the concentration of diluent in the epoxy system.

In the case of E-based epoxy samples, the gradual increase in diluent content from 15 to 25 phr gradually increased the maximum load. Further increase in diluent from 25 to 30 phr led to a fall in maximum load. However, it can be seen that for E-based epoxy samples of different diluent contents, the maximum displacement steadily increased with diluent weight fraction in the epoxy system. The same trend can be observed for L-based epoxy samples as a function of diluent content. An increase in diluent content from 30 to 60 phr gradually enhanced the maximum load on the load–displacement curves of L-type epoxies, and further increase in diluent from 60 to 70 phr gave rise to a decrease in maximum load. Nonetheless, a monotonic increase in the displacement at failure for L-type epoxy samples is clearly obvious as the concentration of diluent was increased from 30 to 70 phr.

The plane-strain critical stress intensity factor (known as fracture toughness) values calculated for E-based and L-based epoxy samples are displayed in Fig. 9. The K_{IC} values for neat E0 and L0 epoxy samples were 1.4 and 1.3 MPa m$^{1/2}$, respectively. For E-based epoxy samples, it can be seen that the fracture toughness gradually increased with the diluent content in the epoxy sample. The same trend is visible for L-based epoxy samples. The data demonstrate that the fracture toughness of L-based epoxies also enhances as a function of diluent concentration in the material. At a given amount of reactive diluent (i.e., 30phr), the
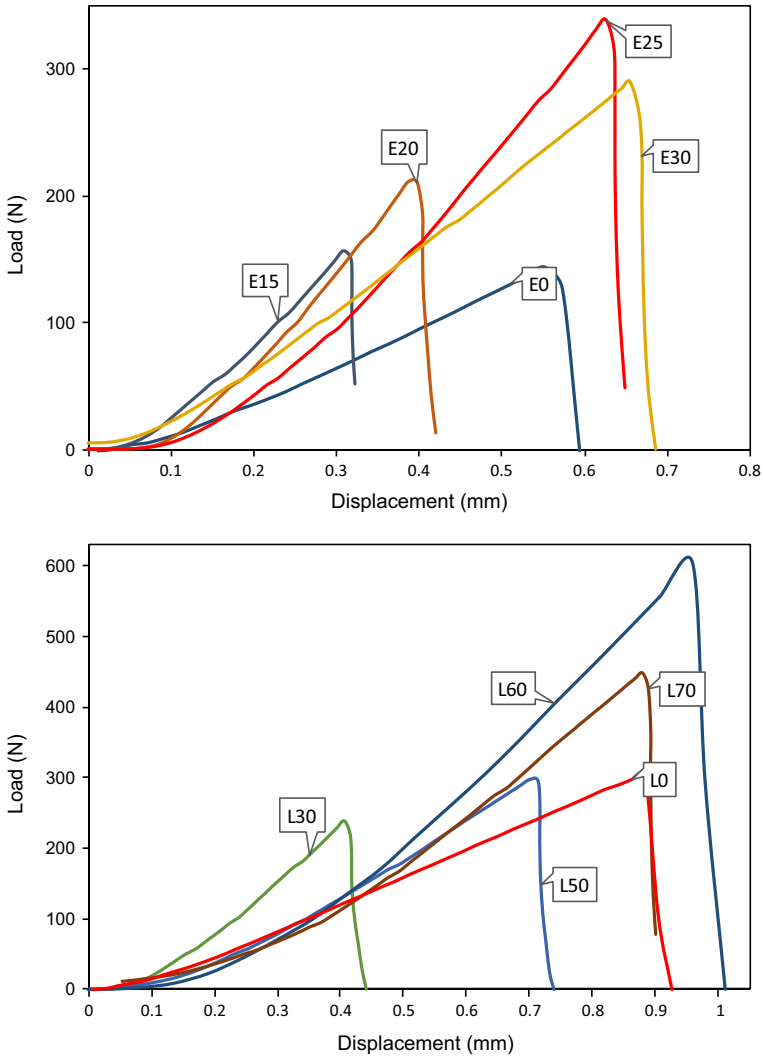
Fig. 8 Load–displacement curves of fracture test for different epoxy samples containing various amounts of reactive diluent

fracture toughness data reveal that the E30 sample has a slightly higher fracture toughness than the L30 sample. The improved fracture toughness of both E- and L-based epoxy samples with diluent content can be attributed to the increased ductility of the resulting epoxy material upon the incorporation of diluent in the material [24–26]. The enhanced ductility with the addition of diluent is undoubtedly due to reduced CLD value of epoxy samples with diluent content. The increased material's ductility is favorable for the activation of higher degree of shear yielding and plastic deformation under the external loads [22, 25, 29]. For
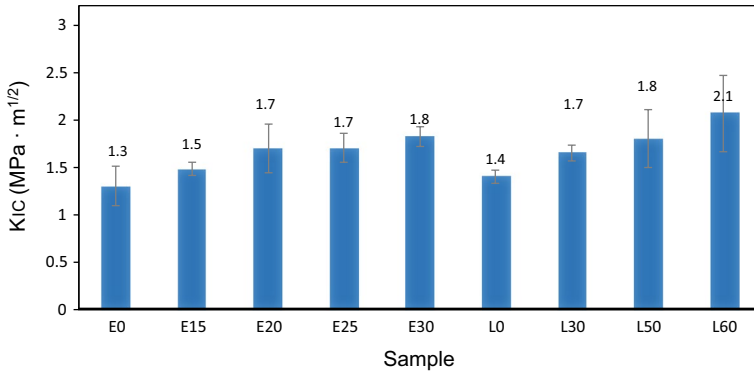
Fig. 9 Fracture toughness (K_{Ic}) values of E- and L-based epoxy resins containing different amounts of reactive diluent
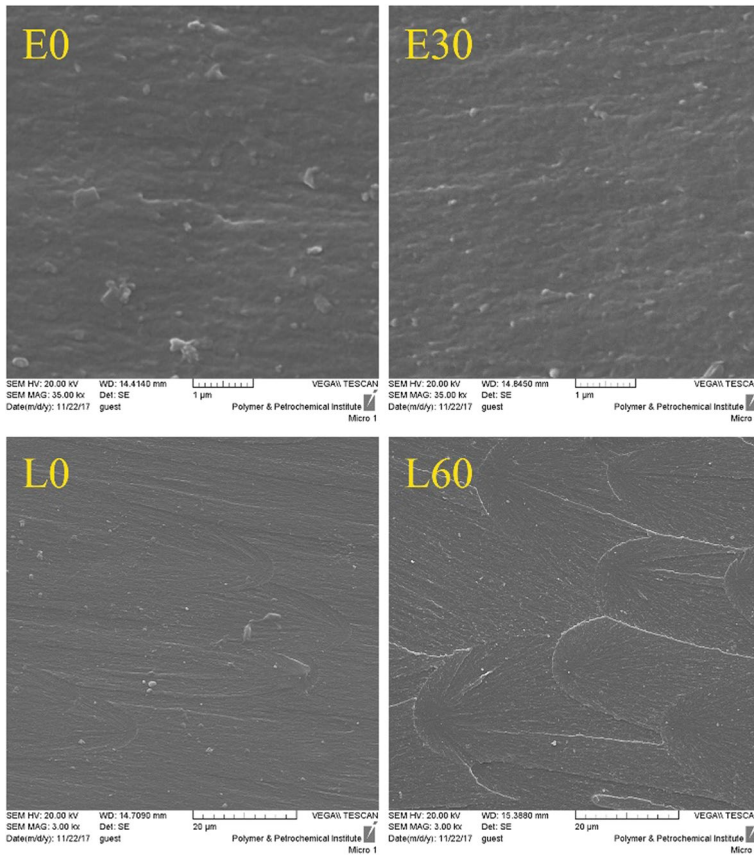

Fig. 10 SEM micrographs taken from the fractured surfaces of different (E0; E30; L0; L60) epoxy samples

diluted samples, the applied fracture stress is dissipated via energy absorption and/or dissipation processes of plastic deformation.

Fractography

The fractured surfaces of the samples were studied via the SEM and AFM analyses. The SEM micrographs taken from the surfaces of the samples obtained after the fracture mechanics tests are shown in Fig. 10. For pure E-type epoxy sample (E0), a smooth fractured surface is apparent, indicating a brittle fracture behavior. For E-based epoxy sample containing 30 wt% reactive diluent also, a smooth fractured surface is obvious. However, there is some evidence of localized plastic deformation on the surface of this sample, suggesting greater amount of energy dissipation during the fracture test compared with the unmodified sample.

For L-type pure epoxy sample in Fig. 10, some evidence of fracture initiation zones is visible on the surface. Lower fracture initiation sites can be seen on the fractured surface of L60 sample, indicating higher fracture resistance of this material during the fracture tests.

Since all the neat and modified L- and E-type epoxy samples exhibited linear load–displacement curves under the fracture tests (Fig. 10), the macroscopic fracture behavior of these samples was of brittle type. As a result, the fractured
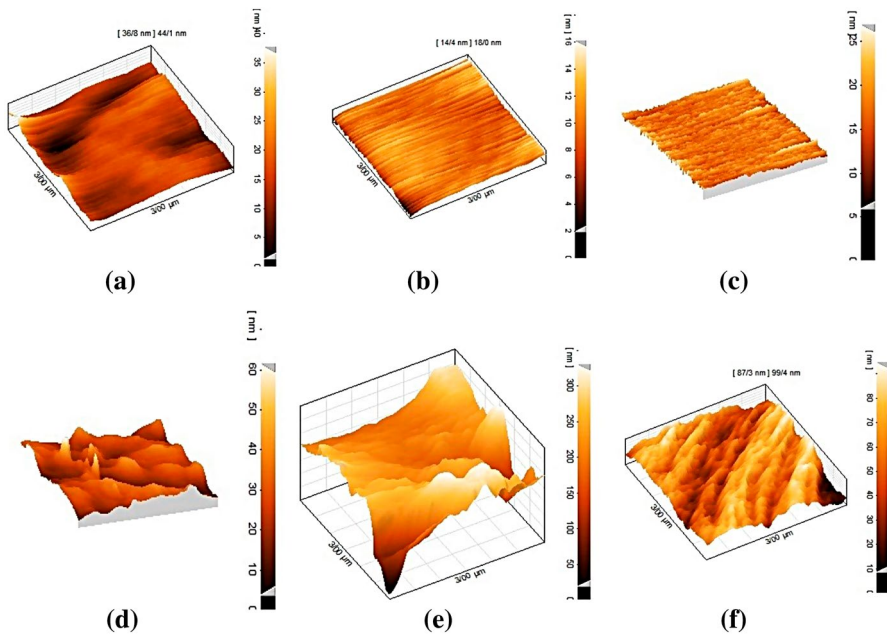

Fig. 11 AFM micrographs taken from the fractured surfaces of different epoxy samples. **a** E20, **b** E25, **c** E30, **d** L30, **e** L50, **f** L70

surfaces of these samples were smooth regardless of the type of the epoxy sample and the extent of the plastic deformation and shear yielding was not significant.

The AFM micrographs taken from the fractured surfaces of some of epoxy samples are shown in Fig. 11. In the case of E-type epoxy samples, the micrographs in Fig. 11a, b reveal that for samples with 20 and 25 phr diluent the fractured surface is very smooth. With an increase in diluent content from 25 to 30 phr, the fractured surface becomes rougher. The increased roughness of fractured surface indicated greater resistance of the material against crack initiation and subsequent propagation, as higher volume of material participates at the deformation process [22, 29, 30]. The fractured surfaces of different L-type epoxy samples are depicted in Fig. 11c, d. As can be seen, the AFM micrographs reveal the significantly rougher fractured surfaces of L-type epoxies compared with E-type samples. The much higher surface roughness is in agreement with the higher fracture toughness of L-type epoxies than the E-type epoxies. It seems that the surface roughness tends to increase with diluent content in the L-type epoxy systems. The much higher roughness of L-type epoxy samples than the E-type epoxies can be attributed to the much higher resistance to crack initiation and subsequent crack propagation during the fracture tests. The increased resistance against fracture is also apparent as larger volumes of material participated in the fracture process which is manifested by the increased surface roughness. The increased fracture resistance for L-type epoxy samples can also be due to higher network cross-link density in these systems.

Conclusions

Two different epoxy resins were modified via the addition of an aliphatic reactive diluent. The effect of diluent content on the viscosity, gel time, chemical resistance, mechanical properties and fracture toughness, was studied. The obtained results led to the following conclusions.

While the viscosity of epoxy samples decreased with diluent content, no significant effect was observed for gel time. The flexural modulus, compressive modulus and ultimate stress gradually declined, while the sample ductility steadily increased with the weight fraction of diluent. A brittle to ductile transition was observed for epoxy samples under the flexural test with the incorporation of diluent into epoxy resins. The introduction of reactive diluent into different epoxy resins reduced the storage modulus at the glassy region and broadened the glass transition region of the epoxy matrices, indicating increased microstructural heterogeneities of epoxy samples upon the addition of diluent. However, no change was found in the glass transition temperature for modified epoxies. The plane-strain fracture toughness improved with diluent content for both epoxy resins, most probably due to improved material's ductility. The obtained results were rationalized in terms of the change in the cross-link density of the epoxy samples with diluent content.

References

1. Petrie EM (2005) Epoxy adhesive formulations. McGraw Hill Professional, New York
2. Vidil T, Tournilhac F, Musso S, Robisson A, Leibler L (2016) Control of reactions and network structures of epoxy thermosets. Prog Polym Sci 62:126–179
3. Hamerton I (1996) Recent developments in epoxy resins. In: Rapra review reports, vol 8. Shawbury
4. Akbari R, Beheshty MH, Shervin M (2013) Toughening of dicyandiamide-cured DGEBA-based epoxy resins by CTBN liquid rubber. Iran Polym J 22:313–3245
5. Ratna D, Banthia AK (2004) Rubber toughened epoxy. Macromol Res 12:11–21
6. Ikram S, Munir A (2012) Mechanical and thermal properties of chemically modified epoxy resin. Open J Synth Theory Appl. 1:36–43
7. Ying WB, Yang HS, Moon DS et al (2018) Epoxy resins toughened with in situ azide–alkyne polymerized polysulfones. J Appl Polym Sci 135:45790
8. Kang S, Kim D, Kim T et al (2017) Toughening epoxy resins with core–shell (HTPB-PMMA/PMA) rubber particles. J Nanosci Nanotechnol 17(10):7429–7435
9. Huang Y, Tian Y, Li Y, Tan X, Li Q, Cheng J, Zhang J (2017) High mechanical properties of epoxy networks with dangling chains and tunable microphase separation structure. RSC Adv 7:49074
10. Kim JR, Kim JJ (2017) Epoxy resins toughened with surface modified epoxidized natural rubber fibers by one-step electrospinning. Materials 10:464. https://doi.org/10.3390/ma10050464
11. Jamshidi H, Akbari R, Beheshty MH (2015) Toughening of dicyandiamide-cured DGEBA-based epoxy resins using flexible diamine rubber. Iran Polym J 24(5):399–410
12. Martinez I, Martin MD, Eceiza A, Oyanguren P, Mondragon I (2000) Phase separation in polysulfone-modified epoxy mixtures: relationships between curing conditions, morphology and ultimate behavior. Polymer 41:1027–1035
13. Giannotti MI, Bernal CR, Oyanguren PA, Galante MJ (2005) Morphology and fracture properties relationship of epoxy-diamine systems simultaneously modified with polysulfone and poly(ether imide). Polym Eng Sci 45:1312–1318
14. Li H, Gan W, Zhao L, Li S (2003) Studies on the phase separation of a polyetherimide modified epoxy resin. VI. Effect of surface energy on reaction-induced phase separation of epoxy resin modified with polyetherimide. J Macromol Sci Part A Pure Appl Chem A 40:833–846
15. Andrés MA, Garmendia J, Valea A, Eceiza A, Mondragon I (1998) Fracture toughness of epoxy resins modified with polyethersulfone: influence of stoichiometry on the morphology of the mixtures. J Appl Polym Sci 69:183–191
16. Grishchuk S, Gryshchuk O, Weber M, Karger-Kocsis J (2012) Structure and toughness of polyethersulfone (PESU)-modified anhydride-cured tetrafunctional epoxy resin: effect of PESU molecular mass. J Appl Polym Sci 123:1193–1200
17. Urbaczewski-Espuche E, Galy J, Gerard J, Pascault J, Sautereau H (1991) Influence of chain flexibility and crosslink density on mechanical properties of epoxy/amine networks. Polym Eng Sci 31(22):1572–1580
18. Tong JD, Bai RK, Zou YF, Pan CY, Ichimura S (1994) Flexibility improvement of epoxy-resin by using polysiloxanes and their derivatives. J Appl Polym Sci 52:1373–1381
19. Zhao F, Sun QC, Fang DP, Yao KD (2000) Preparation and properties of polydimethylsiloxane-modified epoxy resins. J Appl Polym Sci 76:1683–1690
20. Mahnam N, Beheshty MH, Barmar M (2013) Modification of dicyandiamide-cured epoxy resin with different molecular weight of polyethylene glycol and its effect on epoxy/glass prepreg characteristic. High Perform Polym 25:705–713
21. Sprenger S (2013) Epoxy resins modified with elastomers and surface-modified silica nanoparticles. Polymer 54:4790–4797
22. Pearson RA, Yee AF (1989) Toughening mechanisms in elastomer-modified epoxies: Part 3: the effect of crosslink density. J Mater Sci 24:2571–2580
23. Shaw SJ, Tod DA (1989) The effects of cure conditions on a rubber-modified epoxy adhesive. J Adhesion 28:231–246
24. Montserrat G, Andreu P, Cortes Y, Calventus P, Colomer JM (1996) Addition of a reactive diluent to a catalyzed epoxy-anhydride system. I. Influence on the cure kinetics. J Appl Polym Sci 61:1663–1674
25. Harani H, Fellahi S, Bakar M (1999) Toughening of epoxy resin using hydroxyl-terminated polyesters. J Appl Polym Sci 71:29–38

26. Rosu D, Cascaval CN, Rosu L (2000) Curing of para-tert-butylphenol formaldehyde epoxy-acrylic resin in the presence of reactive diluents. Polym Plastic Technol Eng 39(3):553–566

27. Núnez-Regueira L, Villanueva M, Fraga-Rivas I (2006) Effect of a reactive diluent on the curing and dynamo-mechanical properties of an epoxy-diamine system. J Therm Anal Calorim 86(2):463–468

28. Das G, Karak N (2009) Epoxidized seed oil-based reactive diluent for BPA epoxy resin and their green nanocomposites. Prog Organ Coat 66:59–64

29. Bakar M, Szymańska J, Rudecka J, Fitas J (2010) Effect of reactive diluents and kaolin on the mechanical properties of epoxy resin. Polym Compos 18(9):503–510

30. Rahman MM, Hosur M, Zainuddin S, Jajam KC, Tippur HV, Jee-lani S (2012) Mechanical characterization of epoxy composites modified with reactive polyol diluents and randomly-oriented amino-functionalized MWCNTs. Polym Test 31:1083–1093

31. Khalina M, Beheshty MH, Salimi A (2018) Preparation and characterization of DGEBA/EPN epoxy blends with improved fracture toughness. Chin J Polym Sci 36(5):632–640

32. Flory PJ, Rehner JR (1943) Statistical mechanics of cross-linked polymer networks. II. Swelling. J Chem Phys 11:521–526

33. Berahman R, Raiati M, MehrabiMazidi M, Paran R (2016) Preparation and characterization of vulcanized silicone rubber/halloysite nanotube nanocomposites: effect of matrix hardness and HNT content. Mater Des 15:333–345

34. Acebo C, Alorda M, Ferrando F, Fernández-Francos X, Serra A, Morancho JM, Salla JM, Ramis X (2015) Epoxy/anhydride thermosets modified with end-capped star polymers with poly(ethyleneimine) cores of different molecular weight and poly(ε-caprolactone) arms. Express Polym Lett 9:809–823